International Journal of Innovation in Mechanical Engineering and Advanced Materials
Homepage: publikasi.mercubuana.ac.id/index.php/ijimeam
Vol. 8 (No. 2), 2026, pp. 114-129
DOI: 10.22441/ijimeam.v8i2.38756

Article

Finite Element-Based Design and Performance Evaluation of a Chain Conveyor Grid Feeder for Non-Value-Added Reduction in Battery Manufacturing

T. A. Kristiawan [1,*], R. Muzzaqi [1], F. T. Putri [1], and M. Ariyanto [2]

[1]Department of Mechanical Engineering, Politeknik Negeri Semarang, Semarang 50275, Indonesia
[2]Department of Mechanical Engineering, Universitas Diponegoro, Semarang 50275, Indonesia
*Corresponding Author: anggit.kristiawan@polines.ac.id (TAK)

Abstract

Non-value-added (NVA) waiting time in the grid-feeding process of battery manufacturing is caused by the limited capacity of the existing paster machine input conveyor, resulting in production flow interruptions and reduced operational efficiency. Although finite element analysis (FEA) has been widely applied for structural verification of industrial equipment, limited studies have integrated structural validation with operational performance evaluation to address production inefficiencies in battery manufacturing. To address this gap, this study proposes a chain conveyor grid feeder and introduces a cross-platform FEA approach by combining ANSYS Workbench and SolidWorks Simulation with in-situ industrial validation, thereby providing both numerical verification and practical evidence of production performance improvement. This study proposes and evaluates a chain conveyor grid feeder by integrating cross-platform FEA using ANSYS Workbench and SolidWorks Simulation with in-situ operational validation. The methodology includes CAD-based design, linear-static structural analysis under the maximum loading condition using ASTM A36 material properties, followed by fabrication, production-line implementation, and before–after performance evaluation. The FEA results indicate maximum von Mises stresses of 55–57 MPa for the frame subsystem and 60–73 MPa for the conveyor subsystem, both remaining below the ASTM A36 yield strength (250 MPa). The corresponding maximum deflection ranges from 0.41 to 1.09 mm, with minimum safety factors ranging from 2.30 to 4.54, confirming adequate structural reliability. Operational validation further demonstrates that NVA waiting time was reduced from 124.33 s to 0 s, while operator requirements decreased from two to one across two production lines. These findings demonstrate that integrating cross-platform FEA with industrial implementation provides an effective framework for achieving both structural reliability and measurable improvements in production efficiency.

Article Info:
Received: 15 April 2026
Revised: 17 July 2026
Accepted: 18 July 2026
Available online: 23 August 2026

Keywords:
finite element analysis; chain conveyor; grid feeder; non-value-added activities; battery manufacturing

How to cite:

T. A. Kristiawan, R. Muzzaqi, F. T. Putri and M. Ariyanto, " Finite element-based design and performance evaluation of a chain conveyor grid feeder for non-value-added reduction in battery manufacturing," *Int. J. Innov. Mech. Eng. Adv. Mater*, vol. 8, no. 2, pp. 114-129, 2026

1. Introduction

Battery manufacturing comprises a series of interconnected processes, including casting, pasting, formation, and assembly, in which process reliability and throughput are critical to overall production performance. In the pasting stage, grids are coated to produce uniform plates, requiring a continuous and controlled material feeding mechanism (Figure 1(a)). The pasting line consists of grid feeding, the paster machine, roll pressing, drying, finishing, and curing, where the grid feeding subsystem (Figure 1(b)) serves as a critical interface for maintaining process continuity. However, inefficiencies are frequently observed during the grid filling operation, where operators encounter non-value-added (NVA) activities that disrupt material flow and reduce system efficiency. Such NVA conditions are widely recognized as a major source of inefficiency, leading to suboptimal utilization of labor, processing time, and material resources in manufacturing systems [1].

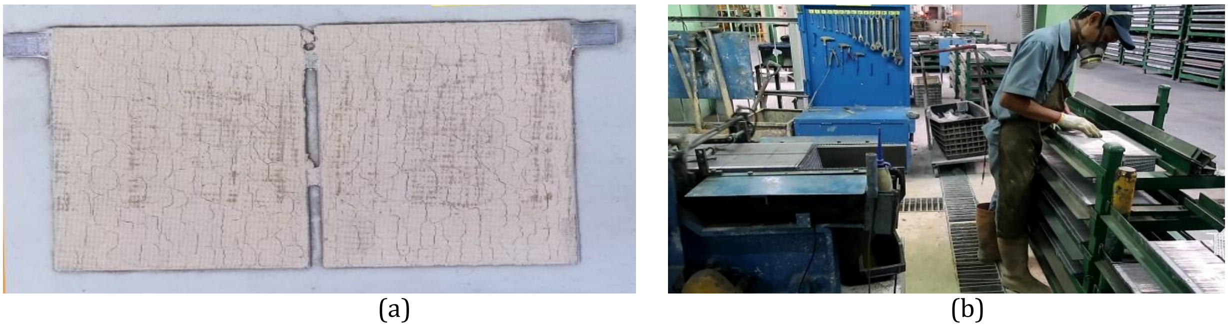

Figure 1. (a) Uniform plate, (b) Grid feeding process.

In practice, these inefficiencies become more pronounced at the operational level, particularly in the grid feeding subsystem. The system operates with two parallel production lines, each assigned to a grid-feeding operator, as illustrated in Figure 2. Waiting-type NVA activities occur when operators must delay the next filling cycle until previously loaded grids are fully processed. This condition is primarily caused by the limited capacity of the existing input conveyor, which is approximately 550 mm in length and accommodates only about 305 grids at a thickness of 1.8 mm, insufficient to handle a full lot of 550 grids. Consequently, a mismatch arises between material supply and process demand. Time study results indicate that the average productive time for grid filling is 30.23 s and 30.82 s for the two lines, while the corresponding NVA waiting time reaches 62.26 s and 62.07 s per cycle, indicating a significant proportion of idle time in the operation.

The presence of non-value-added (NVA) activities adversely affects resource utilization, as operators remain underutilized while labor costs continue to be incurred. Consistent with previous studies, waste in production systems reduces process efficiency and contributes to financial losses [2]. To overcome this issue, a chain-conveyor grid feeder is proposed to increase the grid-filling capacity of the paster machine, enabling a complete production lot to be accommodated in a single loading cycle. The increased conveyor capacity extends the available processing interval, thereby reducing NVA waiting time, improving operator utilization, and enabling a single operator to manage two production lines instead of the previous one-operator-per-line configuration.

In practice, staffing reduction is constrained by operator movement between parallel production lines. The operator requires approximately 20 s to move between lines, resulting in a total travel time of about 40 s per operating cycle, while the available waiting time before the next grid-filling operation is only approximately 60 s. Consequently, the limited capacity of the existing input conveyor cannot provide sufficient processing intervals to support efficient multi-line operation. Increasing the conveyor capacity extends the processing interval, enabling a single operator to effectively manage both production lines.

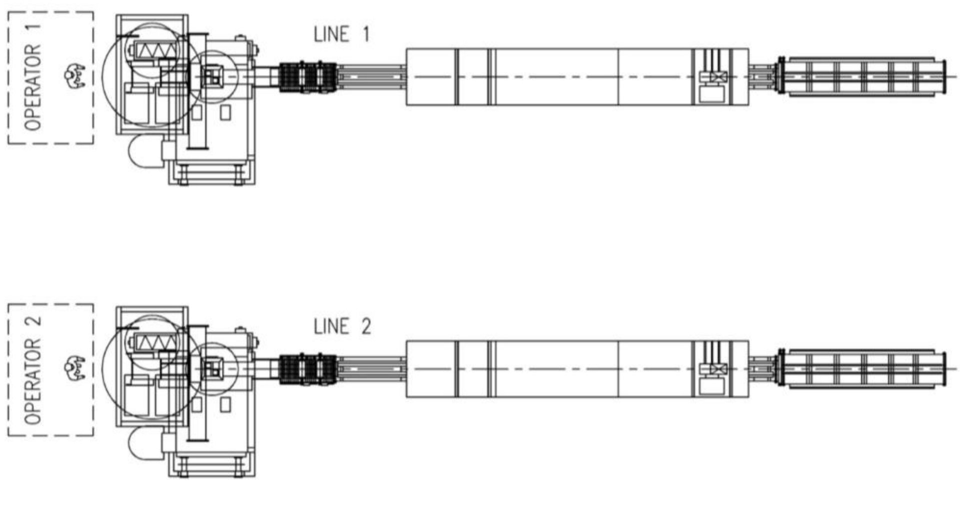

Figure 2. Pasting layout.

Previous studies on waste reduction in manufacturing have extensively applied lean manufacturing approaches to improve process efficiency and resource utilization. Techniques such as Value Stream Mapping (VSM), line balancing, and lean logistics have been widely adopted to identify and eliminate non-value-added (NVA) activities. For example, VSM reduced non-value-added time from 22.77 min to 13.27 min while improving Process Cycle Efficiency (PCE) from 66.10% to 75.29% [3]. Similarly, line balancing and lean logistics have been reported to reduce cycle time and improve resource utilization and warehouse performance [4], [5].

Finite element analysis (FEA) has been widely adopted as a reliable tool for evaluating structural performance and supporting engineering design decisions. Previous studies have demonstrated that FEA can serve as an effective alternative for product prototyping and structural testing, enabling accurate prediction of stress distribution, deformation, and mechanical behavior without extensive physical experimentation [6]. Furthermore, FEA has been successfully applied in structural design optimization to ensure that components can safely withstand applied loads while maintaining efficiency and reliability [7]. For example, dimensional optimization of a conveyor bracket using ABAQUS reduced the maximum stress by approximately 37.32 MPa while improving structural reliability [8]. In addition, a conveyor support frame analyzed using ANSYS Workbench exhibited a maximum von Mises stress of 96 MPa and a maximum deformation of 0.537 mm, confirming its structural safety under operational loads [9]. Furthermore, generative design combined with FEA has also been shown to substantially reduce conveyor bracket mass while maintaining structural safety for industrial applications [10].

Previous studies on waste reduction in manufacturing have predominantly focused on process and organizational improvements, such as line balancing, lean manufacturing, and logistics optimization, to rebalance workloads and streamline material flow. While these approaches have proven effective in improving efficiency, they rarely consider the redesign and implementation of mechanical systems as a primary mechanism for reducing waste at critical process stages. In contrast, studies on conveyor systems using FEA have mainly focused on structural feasibility and design optimization, without integration into real production environments or alignment with operational performance targets. Consequently, these two research domains—process optimization and mechanical system design—are typically addressed independently, resulting in limited integration between structural performance and operational efficiency in manufacturing systems. However, limited studies have integrated structurally validated conveyor system redesign with lean manufacturing implementation to simultaneously improve structural reliability and operational performance in battery manufacturing. Lean manufacturing methods effectively identify and reduce operational waste but cannot by themselves verify the structural integrity of redesigned mechanical systems, highlighting the need to integrate FEA with lean manufacturing.

The novelty of this study lies in integrating the design, finite element-based structural verification, and operational validation of a chain-conveyor grid feeder within a lean manufacturing framework for battery manufacturing. To address this gap, the proposed chain-conveyor grid feeder was designed, structurally verified using cross-platform finite element analysis (ANSYS Workbench and SolidWorks Simulation), and validated through implementation on an actual production line. This study contributes a validated engineering framework for integrating structural design verification with operational performance evaluation and improvement, providing a systematic approach for developing mechanically reliable material handling systems that support lean manufacturing implementation.

The objectives of this study are to evaluate the structural integrity of the proposed chain-conveyor grid feeder under maximum loading conditions, to ensure reliable operation without structural failure or excessive deformation, and to assess its effectiveness in reducing NVA and improving operational efficiency in the grid-feeding process. The analysis is conducted using linear static simulation to evaluate stress distribution, deformation, and safety factor under worst-case loading conditions. In addition, critical regions are identified to ensure that maximum stress and deflection remain within allowable limits.

2. Methods

Following an integrated engineering workflow that combines equipment design, finite-element-analysis (FEA)-based structural verification, fabrication, and experimental validation [11], this research employed an industrial case-study approach to develop and evaluate

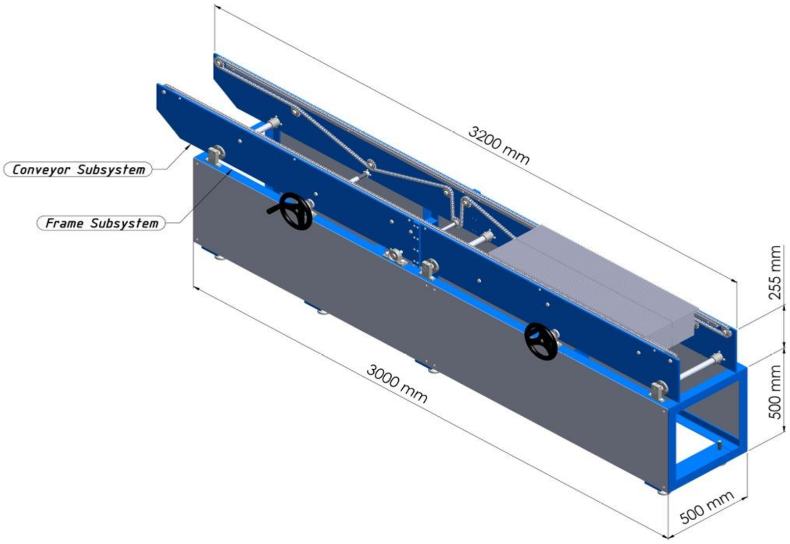

Figure 3. Chain conveyor grid feeder design.

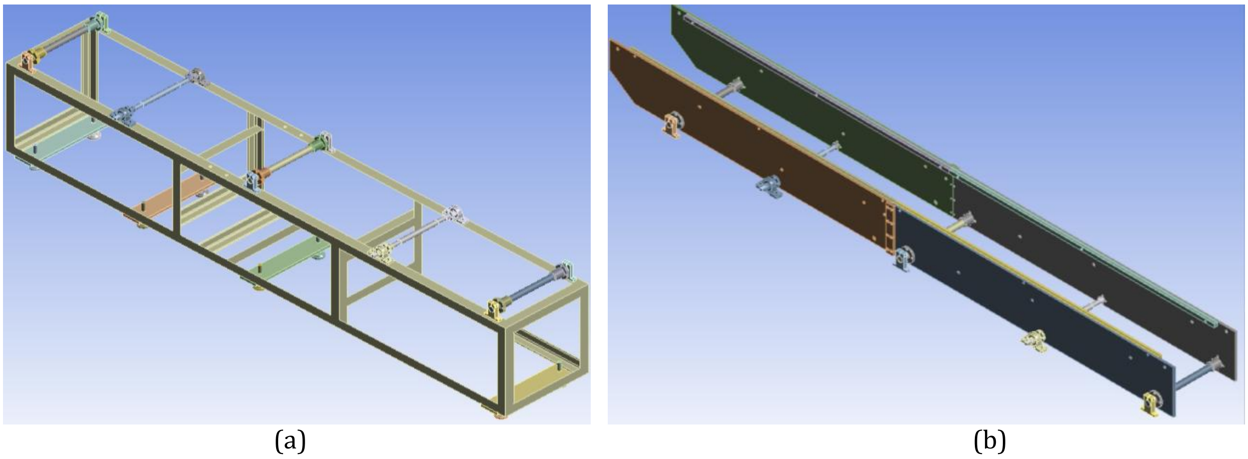

Figure 4. (a) Frame subsystem model, (b) Conveyor subsystem model.

a chain-conveyor grid feeder for battery manufacturing. The research methodology comprised four sequential stages: (1) design of the chain-conveyor grid feeder, (2) structural verification using FEA, (3) fabrication and installation on the production line, and (4) before-and-after performance testing. The study was designed to evaluate the structural reliability of the proposed machine and its effectiveness in reducing non-value-added (NVA) activities and operator requirements. A case-study approach was selected because the proposed equipment was evaluated under actual production conditions, allowing both structural and operational performance to be assessed in its real industrial context.

2.1 Design

The design was developed using SolidWorks Professional 2021 as the 3D CAD (computer aided design) platform to model and verify the fit of all components of the chain-conveyor grid feeder. Finite element analyses were subsequently performed using ANSYS Workbench 2020. Figure 3 shows the completed design. The same CAD model was used as the basis for the FEA geometry, which was divided into two models, namely the frame subsystem and the conveyor subsystem, as shown in Figure 4(a) and Figure 4(b). This partitioning was adopted to simplify model setup and meshing while reducing simulation time.

The FEA geometry was prepared by suppressing noncritical geometric features, such as small fillets and chamfers, that have minimal influence on the overall structural response but may induce excessive local mesh refinement and reduce computational efficiency [12]. The geometry was exported to ANSYS Workbench and SolidWorks Simulation with a consistent coordinate-system orientation. Mass values, component centers of mass, and load-application coordinates were taken directly from the CAD model properties and used as inputs for structural verification.

2.2 Material

All custom components (frame, base plate, chain guides, brackets, and shafts) were manufactured from ASTM A36 in accordance with material standards commonly used in the battery manufacturing industry. ASTM A36 was modeled as homogeneous, isotropic, and linear-elastic. In contrast, standard purchased components used their typical grades: linear bushings used AISI 52100, shaft holders and pillow blocks used AISI 1045, and leveling mounts used ASTM A36. Material properties were applied consistently in ANSYS Workbench and SolidWorks Simulation, with a Young's modulus of 200 GPa, Poisson's ratio of 0.26, and density of 7,850 kg/m^3. The mechanical properties for ASTM A36 steel were taken as an ultimate tensile strength of 400 MPa and a yield strength of 250 MPa [13], [14].

2.3. Finite element analysis

Finite element analysis was performed to evaluate the structural reliability of the frame subsystem and the conveyor subsystem under the worst-case operating load. A linear-static formulation was used because the conveyor speed is low (2.16 m/min), so a static assumption is adequate to represent actual conditions.

The structural analysis is governed by the equilibrium equation of linear elasticity[15]:

$$\nabla . \sigma + f = 0 \tag{1}$$

where σ is the stress tensor and f represents the body force per unit volume. The material behavior follows Hooke's law for isotropic linear elastic materials[15], [16]:

$$\sigma = E . \varepsilon \tag{2}$$

where E is Young's modulus and ε is the strain. The equivalent von Mises stress used to evaluate yielding is expressed as[16]:

$$\sigma_v = \sqrt{\frac{1}{2}[(\sigma_1 + \sigma_2)^2 - (\sigma_1 + \sigma_2)^2 - (\sigma_1 + \sigma_2)^2]} \tag{3}$$

where $\sigma_1, \sigma_2, \sigma_3$ are the principal stresses. This criterion is used to assess whether the induced stress remains below the material yield strength.

The finite element model was developed through geometry preparation, material assignment, contact definition, mesh generation, application of boundary conditions, numerical solution, and postprocessing of the simulation results. The analysis aimed to determine the maximum deformation, maximum von Mises stress, and minimum safety factor for each subsystem under the fully filled worst-case loading condition [17]. Results are presented in figures highlighting the critical regions of the linear-static simulation and in tables comparing the results obtained from the two solvers for each subsystem.

2.3.1 Constraint application

During the constraint application stage, fixed supports were assigned as restraints and loads were applied to the model geometry. Fixed supports were placed on machine regions assumed to remain stationary with no displacement under load. The applied load corresponded to the weight of the grids under a fully filled assumption to represent the worst-case operating condition. This worst-case scenario uses one grid type, with specifications and weight calculations summarized in Table 1.

Table 1. Worst case scenario weight calculation.

Grid Parameter	Value
Grid Thickness	1,2 mm
Grid Weight	125 gram
Total mass at full load	$\left(\frac{\text{Conveyor path length}}{Grid\ Thickness}\right) \times Grid\ Weight$ = $\left(\frac{3200\ mm}{1.2\ mm}\right) \times 125\ gram$ = 333333.3 g

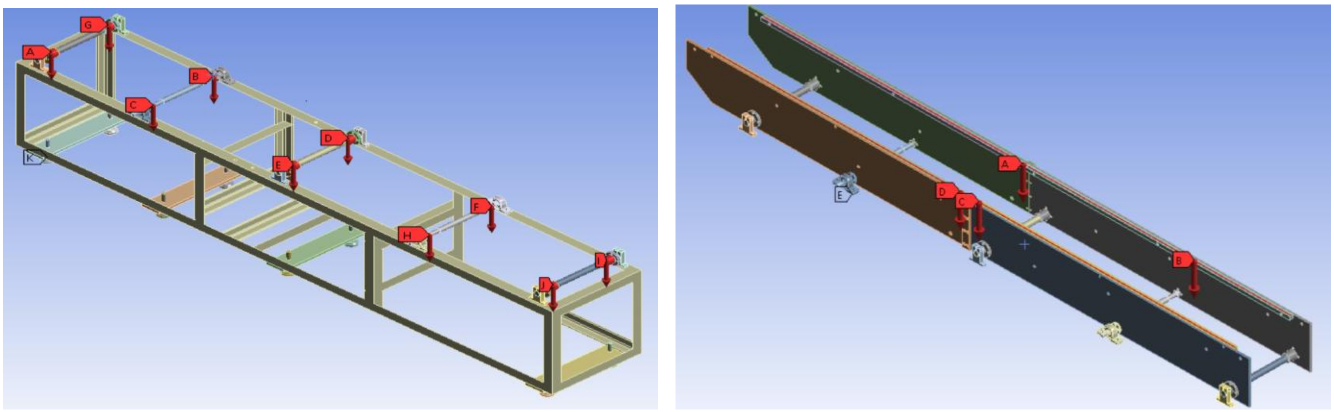

(a) (b)

Figure 5. (a) Frame subsystem boundary condition, (b) Conveyor subsystem boundary condition.

In the frame subsystem simulation, fixed supports were placed at the frame legs. The applied load came from the weight of the grids and the components in the conveyor subsystem. The conveyor subsystem components have a total mass of 147 kg, and the combined gravity load from these components and the grids was 4,712 N. This load was distributed evenly across the connection points between the frame and conveyor subsystems. Details are shown in Figure 5(a).

In the conveyor subsystem simulation, only the grid weight was applied, resulting in a total gravity load of 3,269 N equally distributed to four chain guides (817 N per guide). Fixed supports were assigned at the interfaces between the frame and conveyor subsystems, as illustrated in Figure 5(b). All component connections were modeled as bonded contacts to represent welded joints and tightly clamped bolted joints operating below the slip threshold, thereby preserving the linear-static formulation and focusing on the global structural response.

2.3.2 Meshing

Hexahedral and tetrahedral elements were selected according to the geometric complexity of each part. Hexahedral elements were applied to simpler geometries, whereas tetrahedral elements were used for more complex shapes. The mesh was generated uniformly at first and then locally refined in regions expected to become hotspots.

Mesh sizes were tailored to each component's dimensions, so different parts used different element sizes. To ensure the solution was not sensitive to element size, a stepwise mesh-convergence study was performed with a focus on maximum von Mises stress. Four convergence iterations were run under identical boundary conditions, and the relative change between iterations was computed as a percentage. Convergence was declared when the percent difference in maximum von Mises stress was below 5%.

Table 2. Frame subsystem mesh convergence.

Iteration	Node	Element	von Mises Stress (MPa)
1	411,300	193,632	46.7
2	517,129	245,691	50.23
3	597,322	328,589	53.94
4	587,806	326,932	55.09

Table 3. Conveyor subsystem mesh convergence.

Iteration	Node	Element	von Mises Stress (MPa)
1	188,830	90,570	55.5
2	310,574	131,302	64.67
3	373,017	173,532	72.17
4	516,988	219,562	74.2

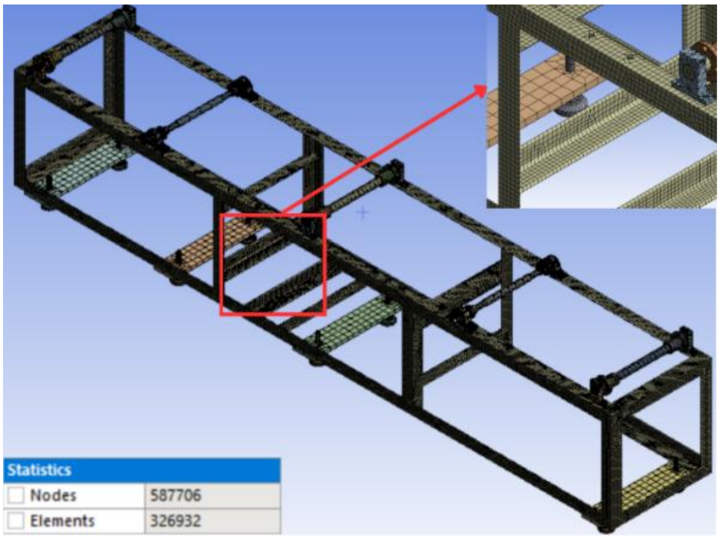

Figure 6. Frame subsystem final mesh.

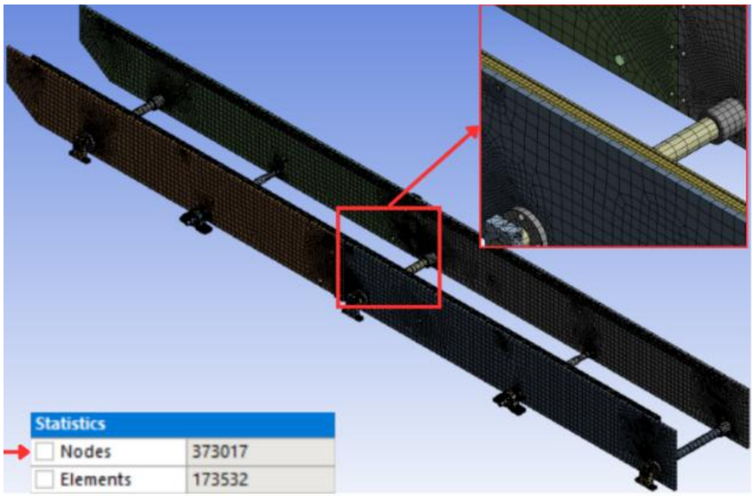

Figure 7. Conveyor subsystem final mesh.

This approach is consistent with a previous study that treated the mesh as converged when the von Mises percent change fell below 5% in their convergence test [18]. Based on Table 2, mesh convergence for the frame subsystem was achieved at the third and fourth iterations, with a percent difference in maximum von Mises stress of 2.08%. Likewise, for the conveyor subsystem, convergence was achieved at the third and fourth iterations with a percent difference of 2.73%, as shown in Table 3. The fourth iteration was adopted as the final mesh for the frame subsystem, with 587,706 nodes and 326,932 elements (Figure 6). For the conveyor subsystem, the third iteration was selected as the final mesh, with 373,017 nodes and 173,532 elements (Figure 7).

2.3.3 Solver and cross validation

Simulations were run in ANSYS Workbench and SolidWorks Simulation under linear-static conditions. Geometry, material properties, boundary conditions, and load magnitudes were aligned so both platforms used equivalent models. Results were compared to three key metrics: maximum deformation, maximum von Mises stress, and minimum safety factor for each subsystem.

A cross-validation table summarizes the side-by-side comparison. The same method has also been carried out in a study comparing deformation in SolidWorks & ANSYS software for the same boundary conditions & loading for three different structural configurations. Overall, this study shows the potential of FEM analysis in improving the design and performance of structures in engineering applications [19].

2.3.4 Acceptance criteria

Structural performance was evaluated using three criteria. The maximum von Mises stress had to remain below the material yield strength specified in the Materials subsection. The minimum safety factor had to meet or exceed the prescribed limits. In all cases, the safety factor was required to be greater than 1.0 to avoid failure [16]. The following ranges summarize commonly used safety-factor values by loading type [20].

Static Load : 1,25 – 2
Dynamic Load : 2 – 3
Shock Load : 3 – 5

Since the proposed chain-conveyor operates at a low conveying speed (2.16 m/min) and was evaluated under a fully loaded stationary condition using linear static analysis, the structural assessment in this study follows the static loading criterion.

The criterion for maximum deflection was functional, and it could not exceed a threshold that would compromise clearance, alignment, or product flow. A previous study indicates that when deformation is very small relative to the overall frame size and can be neglected, the frame stiffness is considered sufficient [21]. These criteria were applied consistently to the frame and conveyor subsystem simulations and they formed the basis for interpreting the results in the next section.

2.4. Fabrication and installation

Fabrication followed the working drawings from the CAD design. After fabrication, dimensions, anchor-hole locations, and inter-component clearances were inspected. Installation connected the chain conveyor to the paster machine so the grids carried by the conveyor could be transferred to the machine. A trial run was then performed with simulated loads to check mechanical stability, chain tension, and product flow.

2.5. Performance testing

Performance testing evaluated the machine in service and its effectiveness in reducing operator NVA. Testing used a before–after design at the grid-feeding station under normal operating conditions. Baseline (pre-installation) measurements were taken on the line in its legacy configuration, and post-installation measurements were taken after the machine was installed.

The recorded variables were productive time, defined as the duration of grid filling to the paster machine, NVA (waiting) duration, and the grid-feeding staffing level. Timing used a stopwatch time study with n = 10 cycles for each condition (pre-installation and post-installation). Measurements were taken by the same observer to minimize bias. Extreme deviations were re-checked with repeat measurements. Data were processed using descriptive statistics by calculating and comparing the mean values for each measured parameter before and after machine implementation**.** The summary results are presented in comparative tables and charts.

3. Results and Discussion

This section presents the results and discussion of the structural verification of the frame and conveyor subsystems using FEA under worst-case loading conditions. The analysis is performed using two simulation platforms, and the results are evaluated based on the criteria defined in the Methods section.

3.1. Stuctural response of the frame subsystem

The simulation results indicate that the frame subsystem operates within safe structural limits under the applied loading conditions. The subsystem exhibits relatively small deformation, with maximum values of 0.58 mm in ANSYS Workbench (Figure 8(a)) and 0.71 mm in SolidWorks Simulation (Figure 8(b)). The maximum deflection occurs at the midspan of the threaded shaft, where bending effects are dominant. However, the deformation remains small relative to the overall structural dimensions, indicating that it does not significantly affect alignment, load transfer, or operational performance. This suggests that the frame subsystem has sufficient stiffness to maintain structural stability. Similar behavior has been reported in previous studies, where small deformation values in structural frames do not significantly influence mechanical performance under operational loads [22], [23].

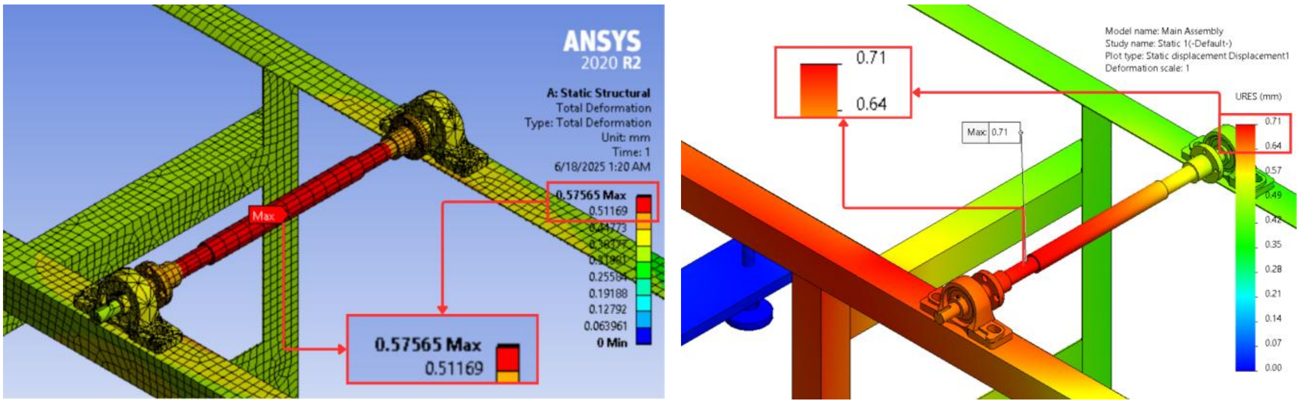

(a) (b)

Figure 8. Deformation results; (a) ANSYS Workbench, (b) SolidWorks Simulation.

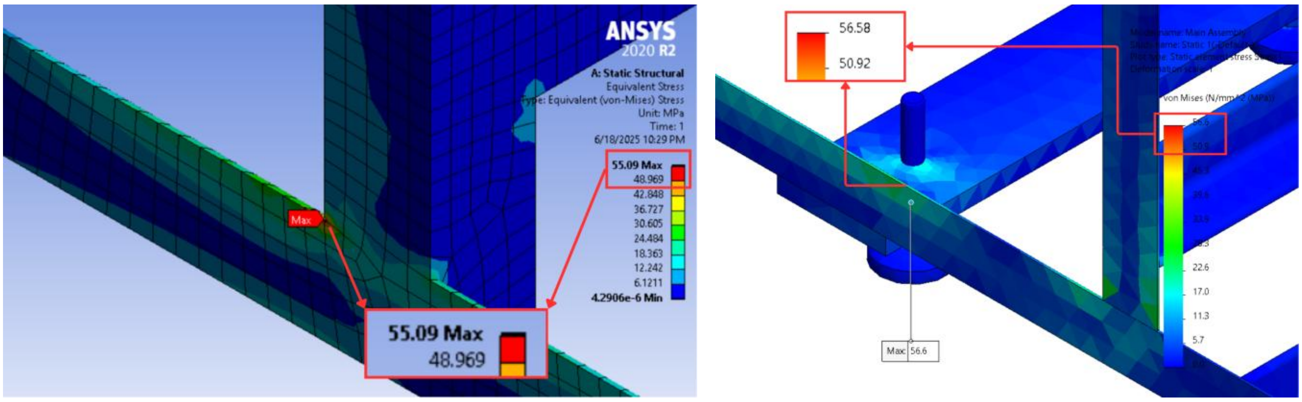

(a) (b)

Figure 9. von Mises stress distribution; (a) ANSYS Workbench, (b) SolidWorks Simulation.

The maximum von Mises stresses are 55.09 MPa in ANSYS Workbench and 56.58 MPa in SolidWorks Simulation (Figure 9(a) and Figure 9(b)), with peak values occurring near the frame joints, indicating localized stress concentration. These values are significantly below the yield strength of ASTM A36 (250 MPa), confirming that the structure operates within the elastic range and is not susceptible to plastic deformation. Previous studies on machine frame structures have demonstrated that stress levels below the material yield strength indicate safe structural performance and adequate load-bearing capacity [24], [25].

The safety factor distribution further supports the structural reliability of the frame subsystem under the worst-case static loading condition. The minimum safety factors are 4.54 in ANSYS Workbench and 2.3 in SolidWorks Simulation (Figure 10(a) and Figure 10(b)), both exceeding the recommended safety-factor range for static loading (1.25–2.00).

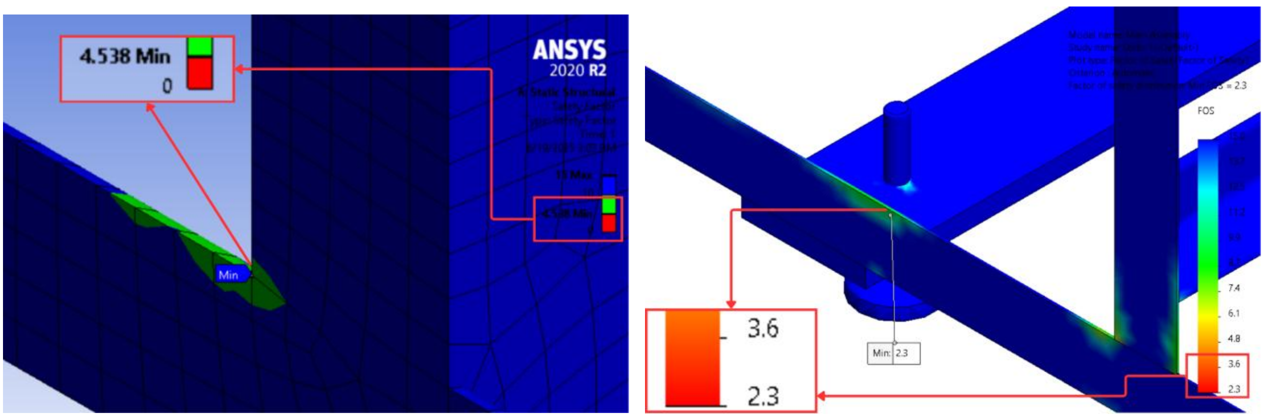

(a) (b)

Figure 10. Safety factor; (a) ANSYS Workbench, (b) SolidWorks Simulation.

These values indicate that the structure can sustain loads significantly higher than the operational requirement. Additionally, most regions exhibit high safety factors, suggesting a conservative design. Similar findings have been reported in structural analyses, where high safety factors indicate reliable performance and provide opportunities for design optimization without compromising safety [22]. Overall, the results confirm that the frame subsystem is structurally safe and reliable under the applied loading conditions.

3.2. Structural response of the conveyor subsystem

The simulation results indicate that the conveyor subsystem maintains structural integrity under the applied working loads. The subsystem exhibits relatively small deformation, with maximum values of 1.09 mm in ANSYS Workbench (Figure 11(a)) and 0.41 mm in SolidWorks Simulation (Figure 11(b)). The maximum deflection occurs at the midspan of the chain-guide components between bolted connections, where bending effects are dominant. However, the deformation remains small relative to the structural dimensions, indicating that it does not significantly affect alignment, load transfer, or operational performance. This suggests that the subsystem has sufficient stiffness to maintain functional stability. Previous studies on conveyor structures have similarly shown that small deformation does not significantly affect system performance and reliability under operational conditions [23], [24].

The maximum von Mises stresses are 73.17 MPa in ANSYS Workbench and 60.06 MPa in SolidWorks Simulation (Figure 12(a) and Figure 12(b)), with peak values located around the bolt holes of the chain-guide components, indicating stress concentration regions. These values are well below the yield strength of ASTM A36 (250 MPa), confirming that the structure operates within the elastic range and is not susceptible to plastic failure. Previous studies have demonstrated that stress levels below the material yield strength indicate that the structure is safe under working loads and can sustain operational conditions without failure [24], [25].

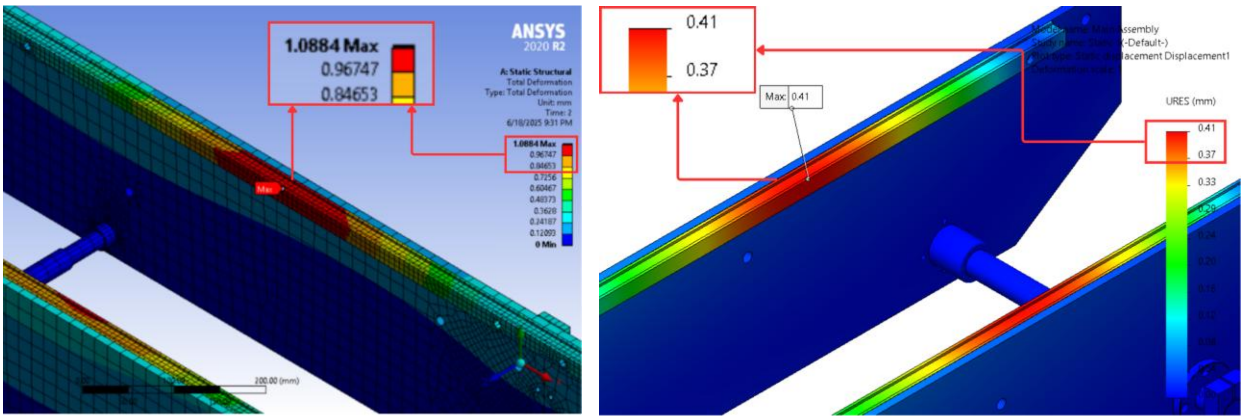

(a) (b)

Figure 11. Deformation results; (a) ANSYS Workbench, (b) SolidWorks Simulation.

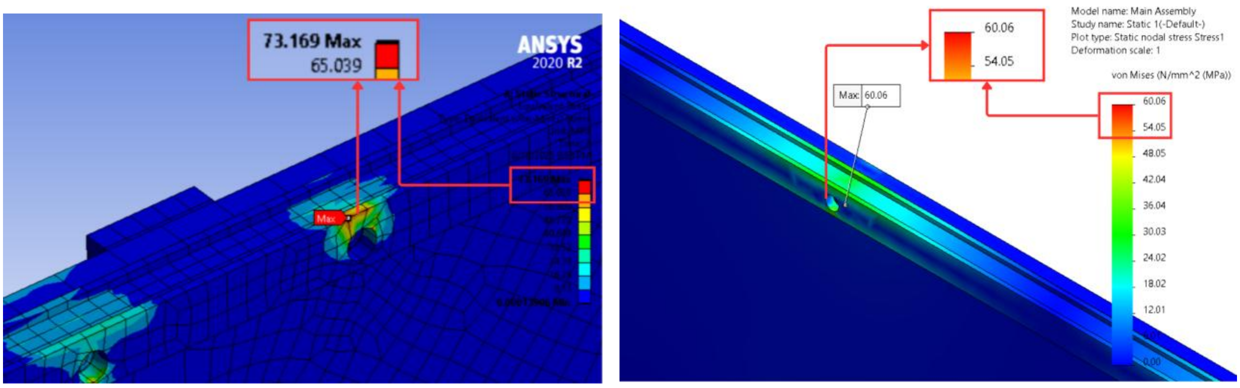

(a) (b)

Figure 12. von Mises stress; (a) ANSYS Workbench, (b) SolidWorks Simulation.

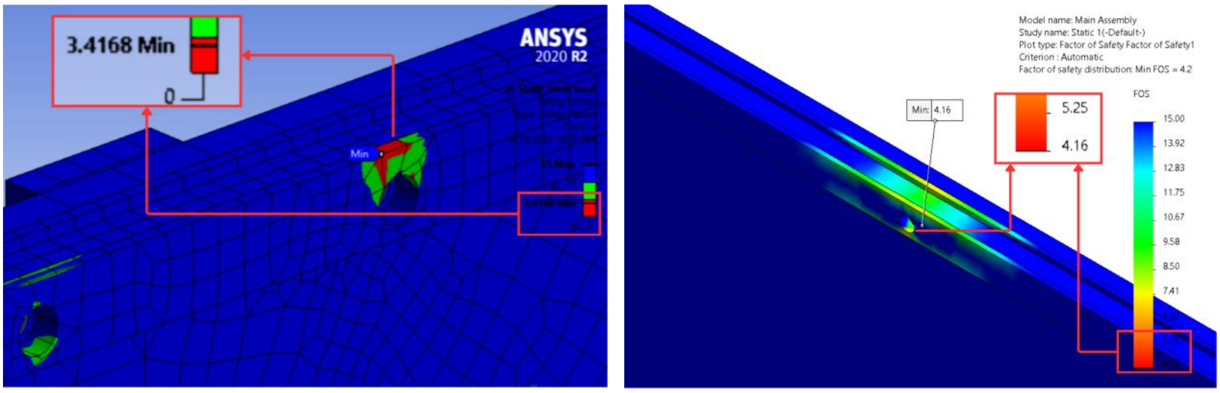

(a) (b)

Figure 13. Safety factor; (a) ANSYS Workbench, (b) SolidWorks Simulation.

The safety factor distribution further confirms the reliability of the design under the worst-case static loading condition, with minimum values of 3.42 in ANSYS Workbench and 4.16 in SolidWorks Simulation (Figure 13(a) and Figure 13(b)), both exceeding the recommended safety-factor range for static loading (1.25–2.00). The lowest values occur at the chain-guide bolt holes, corresponding to the locations of peak stress. These results indicate that the subsystem can sustain loads significantly higher than the operating condition. Moreover, the generally high safety factors suggest a conservative design. Similar findings in structural and conveyor analyses indicate that high safety factors reflect reliable structural performance and potential for optimization without compromising safety [22], [25]. These findings demonstrate that the conveyor subsystem is structurally robust and suitable for continuous operation under working conditions.

3.3. Cross software validation

Cross-platform validation was conducted by comparing the structural analysis results obtained from ANSYS Workbench and SolidWorks Simulation. The comparison focused on the maximum deformation, maximum von Mises stress, and minimum safety factor to evaluate the numerical consistency and reliability of the proposed structural design.

The results in Table 4 and Table 5 show strong agreement between ANSYS Workbench and SolidWorks Simulation, indicating good numerical consistency. The percentage difference in the maximum von Mises stress was 2.67% for the frame subsystem and 17.92% for the conveyor subsystem. Despite the higher percentage difference observed for the conveyor subsystem, both software platforms consistently predicted maximum von Mises stresses well below the ASTM A36 yield strength, resulting in the same engineering conclusion regarding structural safety. Although slight differences are observed, these variations remain within an acceptable range and do not affect the overall structural assessment. Such discrepancies are inherent to the finite element method due to discretization effects, modeling assumptions, and differences in numerical implementation.

Table 4. Frame subsystem FEA result comparison.

Metric	ANSYS Workbench	SolidWorks	Reference Limit	Assessment
Maximum Deformation	0.58 mm	0.71 mm	Within functional limit (no interference)	Safe
Maximum von Mises Stress	55.09 MPa	56.58 MPa	250 MPa	Safe
Minimum Safety Factor	4.54	2.3	1.25-2.00	Safe

Table 5. Conveyor subsystem FEA result comparison.

Metric	Ansys Workbench	SolidWorks	Reference Limit	Assessment
Maximum Deformation	1.09 mm	0.41 mm	Within functional limit (no interference)	Safe
Maximum von Mises Stress	73.17 MPa	60.06 MPa	250 MPa	Safe
Minimum Safety Factor	3.42	4.16	1.25-2.00	Safe

Figure 14. Chain conveyor grid feeder unit.

Table 6. Pre-installation measurement comparison.

Cycle	Grid-Filling Time (s)		Operator NVA Duration (s)	
	Operator 1	Operator 2	Operator 1	Operator 2
1	29.87	30.45	62.36	60.74
2	30.12	31.01	60.97	61.53
3	28.95	31.44	62.13	63.74
4	31.25	29.86	61.55	61.25
5	30.67	32.01	63.3	62.91
6	29.54	31.27	61.24	60.36
7	30.81	29.91	62.59	62.48
8	29.43	32.11	63.16	62.73
9	31.09	30.04	63.51	61.82
10	30.55	30.12	61.77	63.17
Mean	30.23	30.82	62.26	62.07
Overall Mean	61.05		124.33	

However, consistent trends in stress, deformation, and safety factors confirm that both models predict similar structural behavior, indicating reliable results. Previous studies have reported that finite element simulations provide approximate solutions and that variations in results are expected due to discretization and modeling factors inherent in computational analysis [24], [26]. Therefore, these differences do not represent analytical errors but rather demonstrate the robustness of the simulation approach.

Furthermore, the maximum von Mises stresses predicted by both software platforms remain well below the ASTM A36 yield strength (250 MPa), indicating low stress utilization and sufficient structural capacity under the worst-case static loading condition. The safety factors, which exceed the recommended criterion for static loading, further confirm that the proposed design provides adequate structural reliability with appropriate safety margins for practical industrial application.

3.4. Fabrication and installation result

The chain-conveyor grid feeder was successfully fabricated from the CAD working drawings. Figure 14 shows the unit after fabrication and installation on the grid-feeding line. This completed build and installation formed the basis for the subsequent before–after performance test evaluating the machine's effect on operator NVA.

3.5. Comparison of performance test results before and after

A detailed comparison of system performance before and after implementation is presented in Table 6 and Table 7, which show the reduction in operator involvement and the elimination of NVA time across all observed cycles. The performance evaluation results demonstrate a significant improvement in operational efficiency following the implementation of the chain-conveyor grid feeder. The system reduced operator requirements from two to one and eliminated non-value-added (NVA) time from 124.33 s to 0 s, representing a 100% reduction. This indicates that the proposed system effectively removes idle and waiting time, resulting in improved labour utilization and better workflow balance between production lines. These findings are consistent with previous studies reporting that automated material handling systems can reduce idle time, improve cycle time stability, and enhance overall productivity [27]. These improvements enabled continuous material flow without operator interruption, allowing a single operator to efficiently manage two production lines while eliminating NVA waiting time.

Furthermore, the complete elimination of NVA time observed in this study aligns with empirical findings from lean-based process improvements, particularly Value Stream Mapping (VSM), where non-value-added activities such as waiting and unnecessary motion were significantly reduced after system redesign [28].

Table 7. Post-Installation measurement comparison.

Cycle	Conveyor 1 Filling Time (s)	Conveyor 2 Filling Time (s)	Walk to Line 2 (s)	Walk to Line 1 (s)	Operator NVA Duration (s)
1	60.13	62.71	22.34	20.93	0
2	58.75	64.23	18.89	23.48	0
3	63.8	61.44	19.76	24.01	0
4	59.22	57.89	21.23	19.73	0
5	61.72	65.32	24.62	21.54	0
6	58.01	63.54	20.15	18.32	0
7	62.53	59.74	19.34	24.41	0
8	64.1	58.8	23.84	20.57	0
9	57.49	66.21	22.91	19.91	0
10	60.83	60.08	21.01	18.77	0
Mean	60.66	62	21.41	21.17	0
Overall Mean	122.654		42.576		0

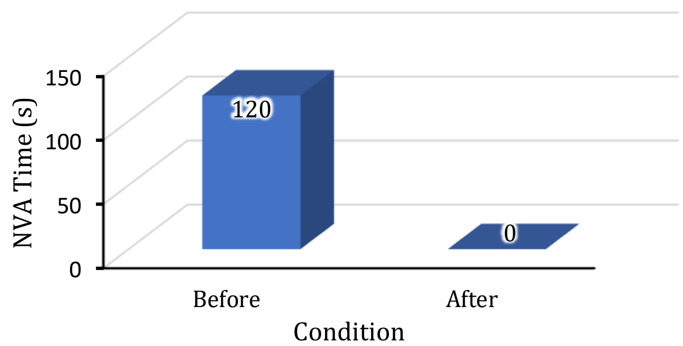

Figure 15. Comparison of non-value-added (NVA) time before and after chain conveyor grid feeder implementation.

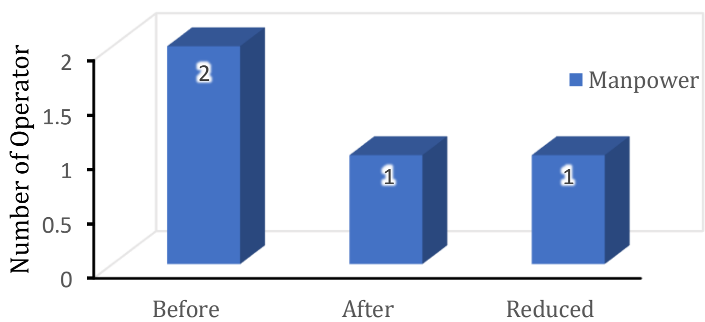

Figure 16. Comparison of operator requirements before and after chain conveyor grid feeder implementation.

The performance improvement is further illustrated in Figure 15 and Figure 16, which present a clear comparison of the reduction in non-value-added time and operator requirements before and after system implementation. Compared to conventional manual handling systems, the proposed design provides a measurable improvement in both process efficiency and manpower utilization, supporting previous research on the effectiveness of conveyor-based system implementation in minimizing bottlenecks and improving production flow [29].

3.6. Discussion

The present study demonstrates that integrating structural verification with industrial implementation provides a practical engineering approach for developing reliable material-handling systems in battery manufacturing. Rather than evaluating structural performance alone, the proposed chain-conveyor grid feeder was successfully implemented under actual production conditions, demonstrating that structural reliability can be effectively translated into measurable operational improvements. This integrated approach supports engineering decision-making by combining numerical analysis with production validation.

From an operational perspective, the redesigned grid feeder enables continuous feeding of one complete production lot, thereby eliminating operator waiting time during the grid-feeding process and improving labor utilization. The improved material flow allows a single operator to continuously manage two production lines while maintaining uninterrupted production. These findings demonstrate that mechanical system redesign can directly support lean manufacturing implementation by eliminating non-value-added activities and improving production efficiency, consistent with previous studies on manufacturing process improvement and waste reduction [29].

Compared with previous studies, most investigations have focused either on structural verification of conveyor systems or on process improvement using lean manufacturing approaches. In contrast, this study integrates cross-validated structural verification with industrial implementation and operational performance evaluation under actual production conditions. The proposed approach not only confirms structural reliability but also demonstrates measurable improvements in production efficiency, thereby providing a more comprehensive framework for evaluating material-handling system redesign in manufacturing environments.

Despite these contributions, several limitations remain. The structural analysis employed a linear-static approach and bonded contact assumptions, which do not consider dynamic loading, impact effects, contact nonlinearity, fatigue, or long-term wear under continuous industrial operation. Future studies should therefore incorporate nonlinear contact analysis [30], dynamic loading analysis [31], fatigue assessment [32], and extended operational validation to further verify the long-term reliability and industrial applicability of the proposed system [33].

4. Conclusions

This study aimed to evaluate the structural integrity and operational effectiveness of a chain-conveyor grid feeder for reducing non-value-added (NVA) activities in battery manufacturing through an integrated approach comprising equipment design, cross-validated finite element analysis (ANSYS Workbench and SolidWorks Simulation), fabrication, industrial implementation, and before-and-after performance evaluation. The results confirm that the proposed chain-conveyor grid feeder is structurally reliable and operationally effective under maximum loading conditions. Cross-validated FEA demonstrates consistent structural behavior between both simulation platforms, with maximum von Mises stresses of 56.58 MPa for the frame subsystem and 73.17 MPa for the conveyor subsystem, maximum deformations of 0.71 mm and 1.09 mm, and minimum safety factors of 2.30 and 3.42, respectively, all satisfying the allowable structural limits. From an operational perspective, the implementation of the proposed system reduced NVA time from 124.33 s to 0 s and decreased operator requirements from two operators to one, thereby improving line balancing and production efficiency in the grid-feeding stage. The main contribution of this study lies in the integration of numerical verification and operational validation. Unlike conventional studies that focus solely on structural feasibility or process improvement, this work provides a combined approach that links cross-validated FEA results with real production data, thereby offering a more comprehensive basis for engineering decision-making. This integrated approach demonstrates that combining structural validation with operational analysis can deliver both technically reliable and practically effective solutions for industrial applications. Despite these contributions, the study is limited to linear-static analysis and simplified contact conditions, which do not capture dynamic loading, impact effects, or long-term fatigue behavior. Future research should therefore consider dynamic analysis, fatigue assessment at critical joints, and extended shop-floor validation to further evaluate long-term performance and reliability.

Acknowledgements

The authors would like to express their sincere gratitude to the industrial partner for providing access, facilities, and support necessary to conduct this research. The identity of the company is withheld for confidentiality reasons.

Declaration of Generative AI and AI-Assisted Technologies in the Writing Process

The author used generative artificial intelligence (AI) tools during the preparation of this manuscript solely to assist with language editing, including grammar improvement, sentence refinement, and enhancement of clarity. All technical content, methodology, analysis, and conclusions were developed, verified, and validated by the author. No AI tools were used to generate research data or scientific results, and the author takes full responsibility for the accuracy, integrity, and originality of the work.

References

[1] S. Chaudhary and M. Choudhary, "Productivity improvement in a small-scale industry using time study," *International Research Journal of Engineering and Technology*, vol. 12, no. 1, pp. 524–527, Jan. 2025. [Online]. Available: https://www.irjet.net/archives/V12/i1/IRJET-V12I179.pdf
[2] M. Boudribila and M. Id Machiche, "Optimizing financial profitability by eliminating waste in industrial processes: A PRISMA systematic review for a profitable company," *International Journal for Multidisciplinary Research (IJFMR)*, vol. 7, no. 4, 2025, doi: 10.36948/ijfmr.2025.v07i04.51555.
[3] D. A. Lubis, S. Pujangkoro, and J. Hidayati, "Lean approach to minimize waste in biscuit production process using value stream mapping method at PT. XYZ," *J. Sist. Tek. Ind.*, vol. 26, no. 2, pp. 120–127, Jul. 2024, doi: 10.32734/jsti.v26i2.13544.
[4] F. Achmadi, B. Harsanto, and A. Yunani, "Improvement of assembly manufacturing process through value stream mapping and ranked positional weight: An empirical evidence from the defense industry," *Processes*, vol. 11, no. 5, Art. no. 1334, May 2023, doi: 10.3390/pr11051334.
[5] C. M. Díaz-Estela, J. D. Atao-Carrasco, and W. D. Calderón-Gonzales, "Lean logistics-based warehouse management model to reduce non-conforming orders in a metal-mechanic SME: A case study in Peru," *International Research Journal of Economics and Management Studies*, vol. 4, no. 4, pp. 173–186, Apr. 2025, doi: 10.56472/25835238/irjems-v4i4p118.
[6] F. P. Kristianto, Z. Amarta, N. Hutasoit, N. Fariz, and F. P. Herinda, "Finite element analysis method as an alternative for furniture prototyping process and product testing," *Int. J. Reconfig. Embedded Syst.*, vol. 14, no. 1, pp. 231–242, Mar. 2025, doi: 10.11591/ijres.v14.i1.pp231-242.
[7] A. M. Ibrahim, A. M. Ali, and H. Kamel, "Design optimization and production of a small-scale semi-trailer chassis for testing," *J. Eng. Appl. Sci.*, vol. 70, Art. no. 35, 2023, doi: 10.1186/s44147-023-00201-z.
[8] M. Y. Zhang, H. D. Zhu, and W. Zhang, "Finite element analysis of belt conveyor bracket," *J. Phys.: Conf. Ser.*, vol. 1748, no. 6, Art. no. 062047, 2021, doi: 10.1088/1742-6596/1748/6/062047.
[9] N. V. Dhandapani, P. Venkateshwaran, J. Ganesh Murali, and V. S. Thangarasu, "A study on linear static structural FEA of a conveyor stand for different stress distribution and shearing deformation," *International Research Journal of Automotive Technology (IRJAT)*, vol. 1, no. 1, pp. 35–38, 2018. [Online]. Available: https://www.mapletreejournals.com/index.php/IRJAT
[10] R. K. A. S. Abdrian, A. Q. Al Jailani, and M. Tauviqirrahman, "Generative design effectivity on belt conveyor for additive manufacturing using finite element method," *International Communication in Computational Mechanics*, vol. 1, no. 1, pp. 14–43, 2025, doi: 10.37934/iccm.1.1.1443.
[11] E. S. Habib and E. Shamso, "A validated workflow for the design and certification of below-the-hook lifting devices integrating finite element analysis and physical proof testing," *Sci. Rep.*, vol. 15, Art. no. 44058, 2025, doi: 10.1038/s41598-025-31175-y.
[12] S. Zhang and G. Guan, "Deep learning-based mesh quality prediction for CAD model defeaturing," in *Mechanical and Aerospace Engineering: Proceedings of the 16th International Conference (ICMAE 2025)*, X. Lei, Ed. Amsterdam, The Netherlands: IOS Press, 2026, pp. 565–573, doi: 10.3233/ATDE260079.
[13] W. D. Callister Jr. and D. G. Rethwisch, *Materials Science and Engineering: An Introduction*, 10th ed. Hoboken, NJ, USA: Wiley, 2018.
[14] ASTM International, *ASTM A36/A36M-19: Standard Specification for Carbon Structural Steel*. West Conshohocken, PA, USA: ASTM International, 2019, doi: 10.1520/A0036_A0036M-19.
[15] O. C. Zienkiewicz, R. L. Taylor, and J. Z. Zhu, *The Finite Element Method: Its Basis and Fundamentals*, 7th ed. Oxford, U.K.: Butterworth-Heinemann, 2013.
[16] R. G. Budynas and J. K. Nisbett, *Shigley's Mechanical Engineering Design*, 11th ed. New York, NY, USA: McGraw-Hill Education, 2020.
[17] Y. Liu, S. Wang, S. Shi, and J. Tan, "Finite element analysis and optimization of automotive disk brakes using ANSYS," *Symmetry*, vol. 18, no. 2, Art. no. 349, 2026, doi: 10.3390/sym18020349.
[18] A. G. Al-labani, R. L. Taner, O. Özdiler, and K. M. Dinçer, "The optimal initial displacement in rotated maxillary incisor teeth with clear aligner in different periodontal conditions: A finite element analysis," *Appl. Sci.*, vol. 15, no. 19, Art. no. 10502, Oct. 2025, doi: 10.3390/app151910502.

[19] P. Bedar and A. C. R., "Design, 3D modelling, and study on L-bracket rib strength through FEM analysis: A comparative study using SolidWorks and ANSYS software," *International Journal of Scientific Research in Science, Engineering and Technology*, vol. 2, no. 1, pp. 677–686, 2016, doi: 10.32628/IJSRSET173391.
[20] R. L. Norton, *Machine Design: An Integrated Approach*, 5th ed. Boston, MA, USA: Pearson Education, 2013.
[21] H. Ma *et al*., "Finite element analysis and optimization for structure of dry ice cleaning machine frame," *Semarak International Journal of Mechanical Precision Engineering*, vol. 2, no. 1, pp. 11–23, Mar. 2025, doi: 10.37934/sijmpe.2.1.1123a.
[22] T. A. Kristiawan, A. D. Alisyafa'at, P. Yanuar, and T. Setiyawan, "Analisa penggunaan support frame lama pada desain baru screw conveyor machine menggunakan metode elemen hingga," *Jurnal Mesin Nusantara*, vol. 6, no. 1, pp. 35–46, Jul. 2023, doi: 10.29407/jmn.v6i1.18847.
[23] Adin and A. A. Saputra, "Design of conveyor using finite element method and finite element analysis," *JTTM: Jurnal Terapan Teknik Mesin*, vol. 6, no. 2, pp. 252–259, Oct. 2025, doi: 10.37373/jttm.v6i2.1633.
[24] W. Wang and X. X. Sun, "Design of automatic deflection correction device and control system for storage belt bin of retractable belt conveyor," *J. Eng. Appl. Sci.*, vol. 72, Art. no. 267, 2025, doi: 10.1186/s44147-025-00807-5.
[25] A. Khoryanton, K. Purbono, P. Yanuar, T. K. Anggit, and C. W. Setiawan, "Design and construction of Atlas Copco bracket set type LE/LT series LT 5-30 to support train Railbus compressor module," *Journal of Engineering Science and Technology*, Special Issue, vol. 18, no. 4, pp. 167–178, 2023. [Online]. Available: https://jestec.taylors.edu.my/
[26] O. Sim, B. C. Jeong, and C. Lee, "Verification, validation, and uncertainty quantification of finite element analysis results for pedicle screw assemblies under ASTM F1717 flexion and extension testing," *Front. Bioeng. Biotechnol.*, vol. 13, Art. no. 1623336, 2025, doi: 10.3389/fbioe.2025.1623336.
[27] A. B. Prasetiyo and K. A. Sekarjati, "Finite element simulation of power weeder machine frame," *Indonesian Journal of Computing, Engineering, and Design (IJoCED)*, vol. 4, no. 2, pp. 25–34, 2022, doi: 10.35806/ijoced.v4i2.291.
[28] T. Nakano and X. Liu, "Guaranteed local error estimation for finite element solutions of boundary value problems," *J. Comput. Appl. Math.*, vol. 425, Art. no. 115061, Jun. 2023, doi: 10.1016/j.cam.2023.115061.
[29] S. S. Rahman, A. Baten, M. Hoque, and Md. I. Mahmud, "Impact of lean manufacturing on productivity and layout design in sewing section of a garment industry," *International Journal of Industrial Management*, vol. 17, no. 3, pp. 152–161, Sep. 2023, doi: 10.15282/ijim.17.3.2023.8955.
[30] J. Bonari, M. Paggi, and D. Dini, "A new finite element paradigm to solve contact problems with roughness," *Int. J. Solids Struct.*, vol. 253, Art. no. 111643, Oct. 2022, doi: 10.1016/j.ijsolstr.2022.111643.
[31] C. Xie, Z. Liu, and M. Xie, "Dynamic response analysis of scraper conveyor under the condition of chain broken," *J. Vibroeng.*, vol. 25, no. 6, pp. 1053–1067, 2023, doi: 10.21595/jve.2023.23192.
[32] D. Patil, "FEA stress determination for weld fatigue using hot-spot stress method: Benchmarking and rail application," *International Journal of Computational Methods and Experimental Measurements*, vol. 12, no. 3, pp. 191–201, Sep. 2024, doi: 10.18280/ijcmem.120301.
[33] H. M. Dara, A. Raut, M. Adamu, Y. E. Ibrahim, and P. V. Ingle, "Reducing non-value added (NVA) activities through lean tools for the precast industry," *Heliyon*, vol. 10, no. 7, Art. no. e29148, Apr. 2024, doi: 10.1016/j.heliyon.2024.e29148.